Ice Melt-Induced Variations of Structural and Functional Traits of the Aquatic Microbial Community along an Arctic River (Pasvik River, Norway)

Maria Papale [1,†], Carmen Rizzo [1,2,†], Gabriella Caruso [1], Stefano Amalfitano [3], Giovanna Maimone [1], Stefano Miserocchi [4], Rosabruna La Ferla [1], Paul Eric Aspholm [5], Franco Decembrini [1], Filippo Azzaro [1], Antonella Conte [6], Marco Graziano [6], Alessandro Ciro Rappazzo [1], Angelina Lo Giudice [1,*] and Maurizio Azzaro [1]

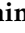1   Institute of Polar Sciences, National Research Council (CNR-ISP), 98122 Messina, Italy; maria.papale@isp.cnr.it (M.P.); carmen.rizzo@szn.it (C.R.); gabriella.caruso@cnr.it (G.C.); giovanna.maimone@cnr.it (G.M.); rosabruna.laferla@cnr.it (R.L.F.); franco.decembrini@cnr.it (F.D.); filippo.azzaro@cnr.it (F.A.); rappale@libero.it (A.C.R.); maurizio.azzaro@cnr.it (M.A.)
2   Stazione Zoologica Anton Dohrn, Department BIOTECH, National Institute of Biology, 98167 Messina, Italy
3   Water Research Institute, National Research Council (CNR-IRSA), 00015 Monterotondo, Italy; stefano.amalfitano@cnr.it
4   Institute of Polar Sciences, National Research Council (CNR-ISP), 40129 Bologna, Italy; stefano.miserocchi@cnr.it
5   Norwegian Institute of Bioeconomy Research (NIBIO), 9925 Svanvik, Norway; paul.eric.aspholm@nibio.no
6   Department of Chemical, Biological, Pharmaceutical and Environmental Sciences, University of Messina, 98166 Messina, Italy; conte.antonella@outlook.com (A.C.); margraziano@unime.it (M.G.)
*   Correspondence: angelina.logiudice@cnr.it; Tel.: +39-090-6015-414
†   Equal contribution as first author.

Abstract: The effects of climate change-induced ice melting on the microbial communities in different glacial-fed aquatic systems have been reported, but seasonal dynamics remain poorly investigated. In this study, the structural and functional traits of the aquatic microbial community were assessed along with the hydrological and biogeochemical variation patterns of the Arctic Pasvik River under riverine and brackish conditions at the beginning (May = Ice-melt (−)) and during the ice-melting season (July = Ice-melt (+)). The microbial abundance and morphometric analysis showed a spatial diversification between the riverine and brackish stations. Results highlighted different levels of microbial respiration and activities with different carbon and phosphorous utilization pathways, thus suggesting an active biogeochemical cycling along the river especially at the beginning of the ice-melting period. At Ice-melt (−), Gammaproteobacteria and Alphaproteobacteria were dominant in riverine and brackish stations, respectively. Conversely, at Ice-melt (+), the microbial community composition was more homogeneously distributed along the river (Gammaproteobacteria > Alphaproteobacteria > Bacteroidetes). Our findings provide evidence on how riverine microbial communities adapt and respond to seasonal ice melting in glacial-fed aquatic ecosystems.

Keywords: microbial abundance; microbial activities; prokaryotic biomass; bacterial diversity; Arctic River; ice melting conditions

1. Introduction

The inputs of glacial and snow meltwaters into Arctic and sub-Arctic rivers are increasing due to the unprecedented effects of global warming on the cryosphere, with repercussions on the river flow dynamics and ecology. Arctic rivers have attracted less attention than Arctic lakes, despite their central role in polar ecosystem functioning by connecting glacier meltwaters to downstream aquatic systems (e.g., estuaries, coastal systems,

fjords), which receive meltwaters, along with newly released particulate matter, nutrients, chemical contaminants, and allochthonous microorganisms [1,2]. Arctic freshwater systems are considered sentinels of climate change [3], and consequently, their microbial communities could be used as indicators of changing conditions [4]. Microorganisms play a pivotal role in such processes and drive the water quality patterns and fluxes of major biogeochemical elements. The Arctic Ocean is subject to large river inputs, which bring low-salinity waters, organic matter and nutrients, and mobilized ancient carbon, with the rising temperatures and permafrost thawing [5]. The increasing riverine inputs and the consequent pulses of organic matter affects the microbial communities, which could respond by changing their structural and functional traits [6,7].

Prediction of how Arctic and sub-Arctic riverine ecosystems will respond to future climate change will derive from a better understanding of the ecological and biogeochemical traits of inhabiting microorganisms, which experience contrasting environmental conditions over the year. It is noteworthy that hydrological connections, local water residence time, and peculiar features (physical-chemical variables, influence of predation or competition) could strongly contribute in shaping the microbial community along the watercourse, by affecting the balance between the seeding of new microbial taxa from multiple sources (e.g., precipitation, soils, cryosphere) and local sorting [8–13].

Here, we coupled hydrological, biogeochemical, and microbiological measurements at spatial and temporal scales to shed light on the ecological factors modulating microbial assembly and structure in a polar river system (Pasvik River, Northern Fennoscandia). Inter- and intra-site variability of environmental conditions and their impact on the microbial community was examined in two periods, corresponding to the initial phase of ice melting (Ice-melt (−), May) and the ongoing ice-melting phase (Ice-melt (+), July). We hypothesize that the aquatic microbial community will show increasingly similar structural and functional traits between the upland and lowland areas at higher levels of hydrological connectivity induced by the ice-melting.

2. Materials and Methods

2.1. Site Description

The Pasvik River is one of the largest rivers in the Northern Fennoscandia on the border area between Finland, Norway, and Russia. The river starts from Lake Inari (Finland) and flows into the Bekfjord (Norway), which is part of the Varangerfjord in the Barents Sea. The total catchment area is 18,325 km². The hydrographic network of the Pasvik river basin is characterized by a large catchment with numerous small lakes and streams in the upland area, and a wide wetland with brackish waters at the lowland area. The annual water level fluctuation is characterized by a high spring flood, increased autumn flow, and periods of low water in summer/autumn and autumn/winter. The river collects snowmelt, with typical riverine waters at the upland side and brackish waters at the lowland side.

2.2. Sample Collection

In the framework of the SpongePOP project, water surface samples (60–100 cm depth) were collected from 9 stations along the Pasvik River by using acid-washed polycarbonate containers during two sampling periods in 2014, representing the beginning (Ice-melt (−); 22–29 May) and the ongoing (Ice-melt (+); 17–24 July) phases of ice-melting [10,14]. Based on their location, the stations were divided into two groups, including riverine (Stations 9, 5, 1, 2, and 8) and brackish sampling sites (Stations 3, 7, 6, and 4) (Figure 1).

At each sampling time, the main physical-chemical parameters of water were examined: Temperature, salinity, total dissolved solids, pH, oxygen saturation, and redox potential. Samples were preliminarily processed (approximately within 2 h) in the laboratory of the NIBIO Svanhovd Research Station (Svanvik, Pasvik Valley), as described in the following sections.
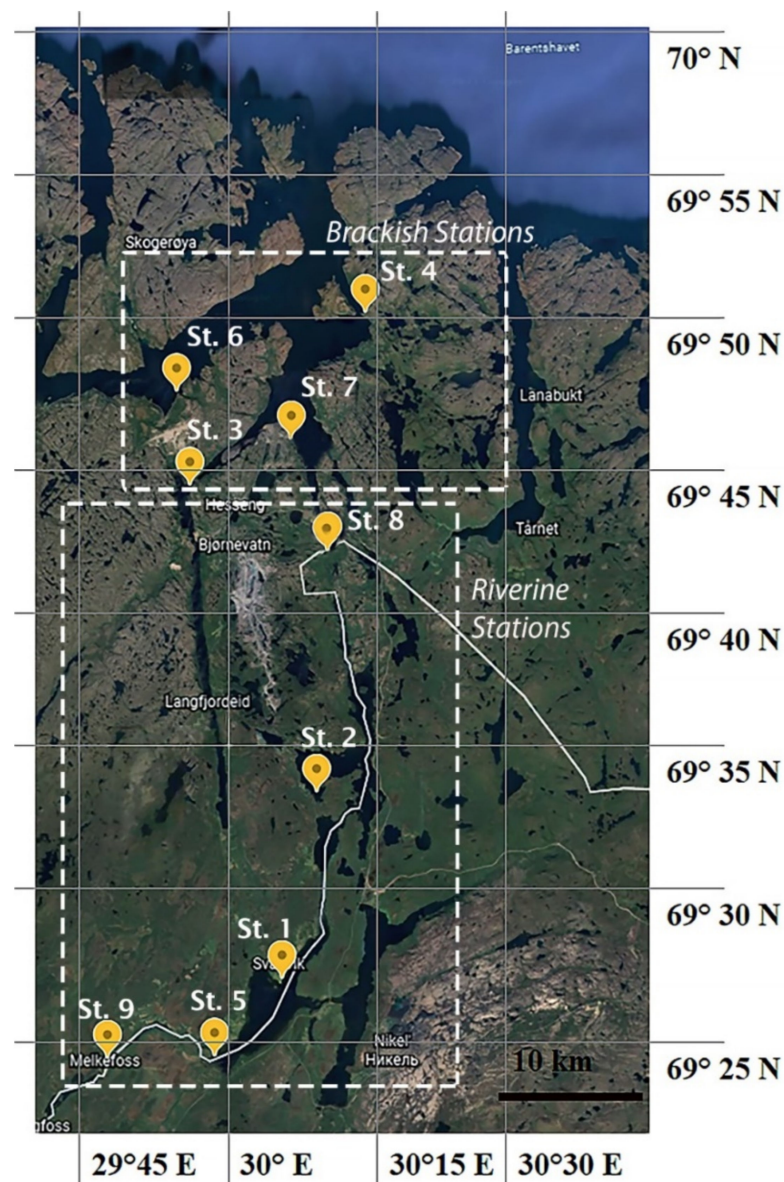
Figure 1. Location of the sampling stations along the Pasvik River.

2.3. Environmental Chemical Variables

2.3.1. Particulate Material

Water samples for total suspended matter (TSM) were filtered on pre-weighed and pre-combusted GF/F filters, rinsed with Milli-Q water and oven-dried (50 °C) overnight, and then weighed to calculate the total suspended matter (mg L^{-1}). Particulate total carbon (Ctot) and organic carbon (POC) were collected filtering on pre-combusted GF/F filters (Whatman, Merck, Rome, Italy) (nominal pore size 0.7 μm) stored at −20 °C until analysis. Both Ctot and POC were analyzed using a FISONS NA2000 Elemental Analyzer (EA; Thermofisher Scientific, Milan, Italy). POC filters were treated with 1.5 N hydrochloric acid to remove the inorganic carbon, and particulate inorganic carbon (PIC) was determined by subtracting the measured particulate organic carbon concentration (POC) from the measured C_{tot} contents and assuming that PIC is composed mainly of calcium carbonate [15].

The stable isotope compositions were measured on a Finnigan DeltaPlus XP mass spectrometer (Thermofisher Scientific, Milan, Italy) directly coupled to a FISONS NA2000 Element Analyzer via a Con*fl*o III interface for continuous flow measurements [16]. The

average standard deviation of each measurement, determined by replicate analyses of the same sample, was $\pm 0.07\%$ and $\pm 0.009\%$ for OC and total nitrogen (PN tot), respectively. All isotopic compositions are presented in the conventional δ notation and reported as parts per thousand (‰). For δ 13 C determinations, the IAEA reference sample IAEA-CH7 (polyethylene, -32.15‰ vs. VPDB) was used for the mass spectrometer calibration. Uncertainties were lower than ± 0.05‰, as determined from routine replicate measurements.

2.3.2. Dissolved Nutrients

Water samples for nutrient determinations (ammonia, NH_4^+, nitrite, NO_2^-, nitrate, NO_3^-, and orthophosphate, PO_4^{3-}) were filtered using GF/F glass-fiber filters and kept frozen ($-20\,^\circ$C). Analytical determinations were performed by a Varian Mod Cary 50 spectrophotometer (Agilent, Santa Clara, CA, USA), according to Strickland and Parsons [17], except for NH_4^+ [18].

2.3.3. Photosynthetic Pigment Contents

Active chlorophyll a (*ch*la) and phaeopigments (phaeophytine and phaeophorbide; phaeo) concentrations were measured by fluorometry [19]. Water samples (0.5–1.0 L) were sequentially filtered through polycarbonate filters (10.0 and 2.0 μm) and then through a Whatman GF/F glass-fiber filter to separate three size fractions: micro-(≥ 10.0 μm), nano- (≥ 2.0 and <10.0 μm), and pico-phytoplankton (≥ 0.2 and <2.0 μm). Filters were immediately stored in aluminum foil at $-20\,^\circ$C until the laboratory analysis. Photosynthetic pigments were extracted in 90% acetone solution and read before and after acidification (HCl 0.5 N). Determinations were carried out with a spectrofluorometer (Varian, mod. Eclipse; Agilent, Santa Clara, CA, USA). Excitation and emission wavelengths (431 and 667 μm, respectively) were selected on the basis of a prescan performed using a solution of chla from *Anacystis nidulans* (Sigma Co., Milan, Italy); chla concentration was calculated according to Lorenzen [20].

2.4. Microbial Abundanc

2.4.1. Total Microbial Cell Abundance by Flow Cytometry (MA-FC)

The abundance of total prokaryotes and pigmented phytoplanktonic microorganisms (i.e., Cyanobacteria, pico-and nano-Eukaryotes) was determined by the flow cytometer A50-micro (Apogee Flow System, Hertfordshire, UK), equipped with a 20 mW Solid State Blue Laser (488 nm). The light scattering signals (forward and side light scatter named FSC and SSC, respectively), red fluorescence (>610 nm), orange fluorescence (590/35 nm), and blue fluorescence (430–470 nm) were acquired and considered for the direct identification and quantification of distinct microbial groups by following harmonized protocols [21]. Total prokaryotes were quantified by following the staining procedure with SYBR Green I (1:10,000 dilution; Life Technologies, code S7563). Thresholding was set on the green channel, and a gating strategy was manually adjusted to exclude most of the unspecific signals according to negative unstained controls. Phycoerythrin-rich (PE) and phycocyanin-rich (PC) Cyanobacteria, pico-and nano-Eukaryotes, were characterized and distinguished according to their pigmentation (i.e., reflecting on different intensities of autofluorescence signals collected at the orange and red channels) and size (i.e., proportionally related to light scatter signals). Thresholding was set on the red channel in order to exclude most of the unspecific signals according to 0.2-μm filtered control water samples. The gating strategy was manually adjusted on the density plots of SSC vs. Red and of Orange vs. Red channels. The volumetric absolute counting was carried out in density plots of SSC vs. the blue channel. Data handling and visualization were performed by the Apogee Histogram Software (version 89.0).

2.4.2. Estimation of Total Prokaryotic Biomass, Cell Volume and Morphotypes by Image Analysis

Total prokaryotic biomass (PB), cell volume (VOL), and morphotypes were estimated after sample fixation with formaldehyde (2% final concentration) and stored in the dark at 4 °C. Appropriate aliquots were filtered on polycarbonate black membranes (porosity 0.2 μm) and stained with 4′,6-diamidino-2-phenylindole (DAPI, Sigma, final concentration 10 μg mL^{-1}) [22] for 20 min. Stained cells were counted by an AXIOPLAN 2 Imaging microscope (magnification: Plan-Neofluar 100 × objective and 10 × ocular; HBO 100 W lamp; filter sets: G365 excitation filter, FT395 chromatic beam splitter, LP420 barrier filter) equipped with the digital camera AXIOCAM-HR (Zeiss, Milan, Italy). Images were captured and digitized on a personal computer using the AXIOVISION 3.1 software. The detailed methodological procedure for the single-cell volume calculation, the volume-to-biomass conversion factor, and the cell carbon content (CCC) are reported in La Ferla et al. [23].

2.5. Microbial Activity Measurements

2.5.1. Extracellular Enzymatic Activity

For the determination of enzymatic activity rates of the microbial community, Hoppe's method [24] was used. Briefly, 10 mL sub-volumes of water samples were added with increasing amounts (from 50 to 300 micromoles) of fluorogenic substrates (Merck Life Science S.r.l., Milan, Italy). The used substrates were leucine aminomethylcoumarine (MCA)-Leu-MCA, 4-methylumbelliferyl (MUF)-beta-d-glucopyranoside, MUF-glu, and MUF-phosphate, specific for leucine aminopeptidase (LAP), beta-glucosidase (beta-GLU), and alkaline phosphatase (AP), respectively.

Measurements of the fluorescence released from the enzymatic hydrolysis of the substrates were performed using a Cary-Varian Eclipse spectrofluorimeter, immediately after substrate addition (time 0) and after 1.5 h of incubation with the substrates at "in situ" temperature, at 380/440 nm (emission/excitation wavelengths) for LAP and at 365/445 nm for beta-GLU and AP. Calibration was performed using known concentrations (between 200 and 800 nmol) of the standards MCA (for LAP) and MUF (for beta-GLU and AP). Measurements gave an estimate of potential enzymatic activity, which was expressed as the maximum velocity (Vmax) of hydrolysis of substrates, in nmol of C or P released per liter and per hour (nmol L^{-1} h^{-1}).

2.5.2. Respiratory Activity

The respiration rates and the consequent metabolic production of CO_2 (R) were measured by the Electron Transport System activity (ETS) assay [25]. This method is based on the conversion of tetrazolium salt into formazan [26,27]. The results were converted into C by using a respiratory quotient of 1 and reported as Vmax (in μgC L^{-1} h^{-1}).

2.6. Phylogenetic Composition of the Bacterial Community

Water samples (between 1.5 and 5.0 L) were filtered through polycarbonate membranes (diameter 47 mm; 0.22 μm) and stored at −20°C until processing. The PowerSoil kit (the MoBio Laboratories Inc., San Diego, CA, USA; Biogenerica, Catane, Italy) was used for DNA extraction. The PCR amplification of the 16S rRNA genes (V1-V2 region) was performed as described by Papale et al. [13]. A two-step PCR protocol was applied to reduce biases in massive sequencing, i.e., a first step of 30 PCR cycles with conventional PCR primers was followed by 6 cycles PCR with barcoded primers for Ion Torrent sequencing using 0.5 μL of first reaction amplicon. PCR reactions (final volume 40 μL) were set up at 0 °C in duplicate by mixing 1 μL of extracted DNA, 0.4 μL of Phusion High-Fidelity DNA polymerase (2U μL^{-1}), 8 μL of Phusion buffer (10×), 1 μL of each dNTP (10 mM), 1 μL of SYBR Green I 25X, and 1 μL of each universal primer (10 μM; 27f: 5′-AGAGTTTGATCCTGGCTCAG-3′; 338r: 5′-GCT GCC TCC CGT AGG AGT-3′). The PCR program was as follows: (1) 98 °C for 1 s; (2) 30 cycles at 98 °C for 10 s, 53 °C for 30 s, and 72 °C for 60 s; (3) 72 °C for 10 s. Amplified products were visualized by electrophoresis agarose gel (1.5%, *w/v*), using

ethidium bromide (EtBr) (1 mg mL^{-1}). Duplicate reactions were pooled and set up under the same conditions to add Ion Xpress barcodes for sample read identification, and IonA and P1 sequences needed in template preparation. The components of the PCR mixture were added to 0.5 µL of pre-amplified DNA to a final volume of 20 µL: 0.2 µL of Phusion High-Fidelity DNA polymerase (2U µL^{-1}), 4 µL of Phusion buffer, 0.5 µL dNTPs (10 mM), 0.5 µL of SYBR Green I 25X, and 0.5 µL of each barcoded primer (10 µM). The reaction was carried out according to the following program: (1) 98 °C for 30 s; (2) 6 cycles at 98 °C for 10 s, 53 °C for 30 s, and 72 °C for 60 s; (3) 72 °C for 10 s. Amplified products were visualized by gel electrophoresis as described above. The purification of PCR products was obtained using the Agencourt AMPure XP kit (Beckman Coulter, Inc., Milan, Italy). Quantification of DNA in purified PCR products was carried out using the Qubit dsDNA HS Assay Kit and the Qubit Fluorometer 2.0 (Invitrogen, Thermo Fisher Scientific, Milan, Italy). Twenty nanograms of each purified product was pooled and checked for size and real concentration with the Agilent TapeStation 2200. The pool was used for emulsion PCR with Ion OneTouch DL. Sequencing was performed on an Ion Torrent Personal Genome Machine™ using the Ion PGM Sequencing 400 Kit and the Ion 314™ chip (all Ion Torrent reagents by Thermo Fischer Scientific, Milan, Italy) following manufacturers' protocols.

Trimmomatic software was used for first quality and trimming steps read portions with a Phred quality score less than 20 per base, and four or more consecutive low-quality base calls were removed (sliding window 4:20) [28]. Subsequent bioinformatics analysis was made with Qiime2 version 2020.8. Then, denoising was carried out with qiime dada2 denoising with the denoisesingle command (using –p-trim-left 15–p-trunc-len 0 –idemultiplexed-seqs) [29]. Quality trimming resulted in approximately 586,086 high-quality reads for 16 samples with an average of 36,630 reads (78.6%) per sample. All samples were included in the downstream quantitative analyses. Sequences were taxonomically classified in QIIME2 (version 2020.8) by SILVA reference files (SILVA release 138 full-length sequences and taxonomy references, release December 2019) using classify-consensusblast. Sequences were clustered into OTUs and taxonomically assigned at 97% identity. The resulting OTU table was normalized to the lowest number of reads among the samples (28,142) for the downstream diversity and quantitative analyses.

2.7. Statistical Analyses

All data were opportunely transformed (log or square root transformation depending on the kind of data) to perform the statistical analysis. The occurrence of significant differences among the station points along the Pasvik River were tested by One-way ANOVA test and post hoc analysis (Tukey test), by comparing the environmental parameters, biological data, and microbial abundance values between samples collected in Ice-melt (−) and Ice-melt (+) periods. Results were considered statistically significant when $p < 0.05$. Correlation coefficients between microbial counts and environmental parameters were calculated to establish the occurrence of significant relationships.

Firstly, the structure of the sampling area according to the environmental parameters recorded at each sampling points in Ice-melt (−) and Ice-melt (+) conditions along the Pasvik River was evaluated. Euclidean distance was calculated, clustering analysis was applied, and a Principal Component Analysis (PCA) was carried out with the obtained resemblance matrix.

As a second step, transformed biological data were processed by calculating the Bray-Curtis similarity. The similarity matrix was used to compute the Non-metric multidimensional analysis (nMDS) on which vectors from diversity data were superimposed, to observe the grouping of the stations according to their biological activities and microbial abundance data in Ice-melt (−) and Ice-melt (+) periods, both separately and together. Finally, all diversity data of abundance at phylum level from Ice-melt (−) and Ice-melt (+) conditions were processed together in a unique nMDS by superimposing the season as the factor and the vectors representing the physical-chemical influences (Primer 7 Plymouth Marine Laboratory, Roborough, UK).

Obtained OTUs for riverine and brackish sampling sites were used to generate Venn diagrams by using the web-based tool 'InteractiVenn' [30].

3. Results

3.1. Physical-Chemical Parameters at Sampling Time

Water temperature was in the range of 2.7–5.5 °C and 14.7–20.6 °C in riverine station samples during the Ice-melt (−) and Ice-melt (+) conditions, respectively. In brackish stations, temperatures ranged 3.2–4.4 °C and 10.4–15.4 °C in the two periods. Salinity ranged between 2.0 and 4.0 in the riverine stations during the Ice-melt (−) season and was almost 0.0 in all stations during the Ice-melt (+) sampling. In the brackish stations, the salinity values ranged between 10.4 and 15.0 in the Ice-melt (−) season and between 5.0 and 30 in the Ice-melt (+) season. Higher values of redox potential were recorded in the Ice-melt (−) season, whereas dissolved solids and oxygen were higher in the Ice-melt (+) than in the Ice-melt (−) season. Finally, pH values were in the ranges 5.9–7.6 and 5.9–8.3 in Ice-melt (−) and Ice-melt (+), respectively (Table 1).

Table 1. Physical-chemical parameters of water samples measured in Ice-melt (−) (May) and Ice-melt (+) (July) seasons.

Stations		Riverine Stations					Brackish Stations			
		St. 9	St. 5	St. 1	St. 2	St. 8	St. 3	St. 7	St. 6	St. 4
Temperature	Ice-melt (−)	5.5	3.7	3.6	2.7	5.5	3.6	3.2	4.4	4.0
	Ice-melt (+)	19.1	20.6	17.2	15.0	14.7	13.0	14.0	10.4	15.4
Salinity	Ice-melt (−)	2.0	3.0	6.0	4.0	4.0	15.0	5.0	15.0	16.0
	Ice-melt (+)	0.0	0.0	0.0	0.0	1.0	15.0	6.0	30.0	17.0
TDS * (ppm)	Ice-melt (−)	23.4	28.3	35.8	18.5	255.0	8.6	1.6 (ppt)	7.5 (ppt)	13.0 (ppt)
	Ice-melt (+)	19.2	173.0	228.0	19.4	2.6	13.5	4.5	19.7	12.9
pH	Ice-melt (−)	5.9	6.4	6.4	7.0	6.0	7.6	6.8	7.7	7.2
	Ice-melt (+)	6.3	7.6	7.2	7.3	5.9	7.8	7.1	8.1	8.3
O$_2$	Ice-melt (−)	87.5	70.5	68	74.9	88.3	93.1	88.5	101.6	102.2
	Ice-melt (+)	83.2	107.9	93.9	94	82.2	96.7	93.8	95	88.2
Redox (mV)	Ice-melt (−)	442.0	175.0	178.0	134.0	252.0	125.0	224.0	140.0	82.0
	Ice-melt (+)	252.0	246.0	198.0	207.0	110.0	37.0	93.0	86.0	81.0

* TDS, Total Dissolved Solids.

3.2. Environmental Chemical Variables

3.2.1. Particulate Material

Total suspended matter (TSM) ranged from 0.35 (at St. 2) to 33.53 mg L^{-1} (at St. 2) at riverine stations and from 0.98 (at St. 3) to 33.30 mg L^{-1} (at St. 4) at brackish stations. The mean TSM value was 4.3 and 11.0 mg L^{-1} in Ice-melt (−) and Ice-melt (+) seasons, respectively.

POC ranged between 153.38 (at St. 2) and 819.49 µg L^{-1} (at St. 5) at riverine stations, and between 120.70 (at St. 3) and 1443.75 µg L^{-1} (at St. 4) at brackish stations. The mean POC value was 366.5 µg L^{-1} in the Ice-melt (−) season and 578.1 µg L^{-1} in the Ice-melt (+) season. In general, samples collected in the Ice-melt (+) season exhibited higher TSM and OC values than in the Ice-melt (−) one.

The range of C/N molar ratios did not differ significantly between seasons, with a mean ratio of 6.7 and 7.0 in Ice-melt (−) and Ice-melt (+) seasons, respectively.

Particulate inorganic carbon (PIC) ranged between 7.43 (at St. 8) and 136.59 µg L^{-1} (at St. 5) at riverine stations and between 1.01 (at St. 3) and 131.07 µg L^{-1} (at St. 7) at brackish stations. The mean value was 61.2 µg L^{-1} (2.3%) in the Ice-melt (−) season and 54.2 µg L^{-1} (1.2%) in the Ice-melt (+) season, showing a slight reduction.

δ^{13}POC values ranged between −31.66 (at St. 2) and −24.53 ‰ (at St. 1) at riverine stations, and between −28.04 (at St. 7) and −24.27 ‰ (at St. 6) at brackish stations. The mean δ^{13}POC value was −28.8 ‰ in the Ice-melt (−) season and −25.8 ‰ 1 in the Ice-

melt (+) season. In general, samples collected at brackish stations showed an increase of $\delta 13$ POC signatures.

TSM and POC values were significantly correlated ($r^2 = 0.61$; $p < 0.01$) (Table 2).

Table 2. Environmental chemical variables in water samples collected in May (Ice-Melt (−)) and July (Ice-Melt (+)) 2014 along the Pasvik River.

Parameter *			Riverine Stations					Brackish Stations			
			St. 9	St. 5	St. 1	St. 2	St. 8	St. 3	St. 7	St. 6	St. 4
Particulate matter	TSM (mg L^{-1})	Ice-melt (−)	1.75	3.2	4.15	0.35	1.175	5.07	5.35	15.25	2.10
		Ice-melt (+)	1.49	5.57	6.725	33.53	14.42	0.98	1.49	1.26	33.30
	POC (µg L^{-1})	Ice-melt (−)	243.61	504.78	594.95	153.38	221.31	225.76	583.96	560.09	211.04
		Ice-melt (+)	242.25	819.49	722.39	725.72	740.90	120.70	159.67	228.33	1443.75
	δ^{13} POC (‰)	Ice-melt (−)	−26.66	−29.69	−30.14	−31.66	−31.58	−27.48	−28.04	−27.26	−26.43
		Ice-melt (+)	−27.78	−25.62	−24.53	−28.39	−25.11	−25.22	−25.60	−24.27	−25.77
	PN tot (µg L^{-1})	Ice-melt (−)	43.19	90.93	128.86	27.72	36.95	36.91	102.47	95.37	33.38
		Ice-melt (+)	47.65	161.54	119.15	90.90	102.49	25.55	31.93	41.40	197.52
	Ctot (µg L^{-1})	Ice-melt (−)	314.84	571.96	717.68	180.18	228.76	226.77	715.02	680.85	213.87
		Ice-melt (+)	271.98	956.08	845.23	780.22	748.33	134.33	194.15	235.33	1525.50
	PIC (µg)	Ice-melt (−)	71.23	67.18	122.72	26.80	7.45	1.01	131.07	120.76	2.84
		Ice-melt (+)	29.73	136.59	122.83	54.50	7.43	13.63	34.47	7.01	81.75
	POC (%)	Ice-melt (−)	13.92	15.77	14.34	43.82	18.84	4.45	10.92	3.67	10.05
		Ice-melt (+)	16.25	14.70	10.74	2.16	5.14	12.27	10.72	18.12	4.34
	PN tot (%)	Ice-melt (−)	2.47	2.84	3.11	7.92	3.14	0.73	1.92	0.63	1.59
		Ice-melt (+)	3.20	2.90	1.77	0.27	0.71	2.60	2.14	3.29	0.59
	PIC (%)	Ice-melt (−)	4.07	2.10	2.96	7.66	0.63	0.02	2.45	0.79	0.14
		Ice-melt (+)	1.99	2.45	1.83	0.16	0.05	1.39	2.31	0.56	0.25
	C/N molar/ratio	Ice-melt (−)	6.58	6.48	5.39	6.45	6.99	7.14	6.65	6.85	7.38
		Ice-melt (+)	5.93	5.92	7.07	9.31	8.43	5.51	5.83	6.43	8.53
Chlorophyll-a content	*Chl*-a (µg L^{-1})	Ice-melt (−)	1.609	0.953	1.961	0.828	1.181	0.951	2.347	1.432	0.638
		Ice-melt (+)	1.495	1.298	1.027	0.826	0.854	1.179	0.754	0.455	1.860
	Pheo (µg L^{-1})	Ice-melt (−)	0.519	0.464	0.796	0.150	0.417	0.426	0.673	0.196	0.824
		Ice-melt (+)	0.549	1.970	0.345	0.457	0.643	0.900	0.313	0.287	0.728
Dissolved nutrients	PO$_4^{3-}$ (µM)	Ice-melt (−)	0.061	0.704	0.861	0.282	0.078	0.164	0.080	0.086	0.091
		Ice-melt (+)	0.013	0.055	0.032	0.029	0.013	0.056	0.027	0.026	0.017
	NH$_4^+$ (µM)	Ice-melt (−)	2.565	1.482	1.7	0.517	0.464	1.866	0.651	1.407	0.783
		Ice-melt (+)	1.760	0.828	0.817	0.449	1.403	6.820	0.909	0.840	3.554
	NO$_3^-$ (µM)	Ice-melt (−)	0.157	0.023	0.487	2.171	2.494	0.474	0.451	0.8	0.335
		Ice-melt (+)	0.435	0.448	0.656	0.288	0.208	1.179	0.253	0.392	0.462
	NO$_2^-$ (µM)	Ice-melt (−)	0.001	0.011	0.023	0.055	0.001	0.026	0.001	0.015	0.024
		Ice-melt (+)	0.021	0.039	0.032	0.051	0.012	0.108	0.002	0.002	0.013

* TSM, Total Suspended Matter; POC, Particulate Organic Carbon; Particulate Nitrogen (PN); Particulate Inorganic Carbon (PIC); Chl-a, chlorophyll-a content; Pheo, pheopigments.

3.2.2. Dissolved Nutrients

NH$_4^+$ concentrations were almost always below 2.6 µM, except in the Ice-melt (+) season at brackish St. 3 and St. 8 (6.820 and 3.554 µM, respectively).

NO$_2^-$ values were very low, showing small variations along the river during both seasons (Ice-melt (−) season, 0.001–0.055 and Ice-melt (+) season, range 0.002–0.108 µM).

NO$_3^-$ concentrations, generally below 1 µM, were slightly higher in the Ice-melt (+) season. Exceptions were the riverine St. 2 and St. 8 with NO$_3^-$ values over 2 µM.

PO$_4^{3-}$ values were higher at all stations in the Ice-melt (−) season (range 0.061–0.861 µM) than in the Ice-melt (+) season (range 0.013–0.056 µM). The maximum values of orthophosphates were determined in the riverine St. 5 and St. 1 (0.704 and 0.861 µM, respectively) (Table 2).

3.2.3. Photosynthetic Pigments

The mean *chl*-a concentration, although with large variations, was quite similar at riverine and brackish sites (1.45 and 1.34 µg L^{-1}, respectively) in the Ice-melt (−) season, with the maximum value (i.e., 2.347 µg L^{-1}) that was found at the brackish St. 7. The size-fraction distribution showed a slightly higher percentage (i.e., 47%) of micro-phytoplankton in riverine than in brackish sites (47 vs. 42%, respectively), whereas pico-phytoplankton was constant (28–29%) in all sites (Table 2 and Supplementary Figure S1).

In the Ice-melt (+) season, mean chla concentration was similar at riverine and brackish stations, with an average concentration of 1.13–1.07 µg L^{-1} (at riverine and brackish stations, respectively), with the maximum value of 1.860 µg L^{-1} that was recorded at the brackish St. 7. The size-fraction distribution found in the Ice-melt (+) season was very similar to that of the Ice-melt (−) season, i.e., the percentage of micro-phytoplankton was slightly higher at riverine than brackish stations (48% vs. 41%, respectively), whereas the pico-phytoplankton was around 29% at all stations. As for the Ice-melt (−) season, nano-phytoplankton was lower at riverine stations.

3.3. Estimation of Microbial Abundance and Morphometric Traits

3.3.1. Total Microbial Cell Abundance by Flow Cytometry (MA-FC)

The microbial community was dominated by non-pigmented heterotrophic microorganisms, including prokaryotic (5.6 ± 2.9 × 10^5 cells mL^{-1}) and eukaryotic cells (1.4 ± 0.5 × 10^4 cells mL^{-1}), with no significant differences between the tested conditions (i.e., riverine vs. brackish; Ice-melt (−) vs. Ice-melt (+)). The pigmented photoautotrophic microorganisms, including Cyanobacteria (mainly represented by PE-rich cells), Pico-, and Nano-Eukaryotes, reached higher and more variable values at low ice-melting levels (i.e., Ice-melt (−) > Ice-melt (+); $p < 0.05$) (Table 3).

Table 3. Microbial cell abundances determined in May (Ice-melt (−)) and July (Ice-melt (+)) by flow cytometry in the Pasvik River.

Microbial Abundance		Riverine Stations					Brackish Stations			
		St.9	St.5	St.1	St.2	St.8	St.3	St.7	St.6	St.4
Heterotrophs (Prokaryotes) (10^5 cells mL^{-1})	Ice-melt (−)	2.09	8.56	10.3	1.42	3.77	4.63	5.13	6.79	3.57
	Ice-melt (+)	5.87	15.3	5.54	4.15	6.53	5.55	3.94	3.64	7.15
Heterotrophs (nano-plankton) (10^4 cells mL^{-1})	Ice-melt (−)	1.24	2.46	2.93	1.30	0.97	1.51	1.94	1.02	0.79
	Ice-melt (+)	1.24	1.37	1.41	0.99	1.49	1.68	0.86	1.22	1.33
Autotrophs (PE-rich Cyanobacteria) (10^3 cells mL^{-1})	Ice-melt (−)	0.39	3.27	43.6	3.87	0.45	15.5	1.74	1.66	3.20
	Ice-melt (+)	0.58	0.37	0.18	0.48	0.28	0.03	0.09	0.01	0.07
Autotrophs (PC-rich Cyanobacteria) (10^2 cells mL^{-1})	Ice-melt (−)	0.70	0.56	14.2	1.47	0.68	2.40	3.85	0.89	0.56
	Ice-melt (+)	0.40	0.74	0.59	0.40	0.26	0.11	0.11	0.14	0.26
Autotrophs (pico-eukaryotes) (10^2 cells mL^{-1})	Ice-melt (−)	2.79	3.90	66.9	3.01	2.40	15.4	26.7	5.06	2.81
	Ice-melt (+)	1.82	4.54	3.22	2.42	1.26	1.05	0.55	0.51	2.27
Autotrophs (nano-plankton) (10^2 cells mL^{-1})	Ice-melt (−)	0.74	1.85	17.7	1.17	0.52	14.9	4.22	3.68	3.00
	Ice-melt (+)	0.59	2.53	3.00	1.34	0.37	0.63	0.25	0.59	6.07

3.3.2. Cell Volume, Prokaryotic Biomass, and Morphotypes by Image Analysis

Generally, cell lengths varied between 0.44 and 0.94 µm and widths between 0.26 and 0.34 µm. Cell volumes were characterized by very small cells that ranged from 0.004 to 0.128 µm^3 with a mean value of 0.037 ± 0.034 µm^3. In both periods, the mean cell

volumes varied in a similar range with cell larger sizes at the brackish stations (mean value 0.040 ± 0.028 μm^3) (Table 4).

Table 4. Morphometric and morphological traits of prokaryotic cells in water samples collected in May (Ice-Melt (−)) and July (Ice-Melt (+)) 2014 along the Pasvik River.

Morphometric Traits		Riverine Stations					Brackish Stations			
		St. 9	St. 5	St. 1	St. 2	St. 8	St. 3	St. 7	St. 6	St. 4
Mean lenght (μm)	Ice-melt (−)	0.47	0.55	0.55	0.56	0.52	0.62	0.48	0.61	0.63
	Ice-melt (+)	0.45	0.49	0.94	0.64	0.44	0.59	0.65	0.78	0.68
Mean width (μm)	Ice-melt (−)	0.31	0.34	0.29	0.32	0.31	0.32	0.32	0.30	0.34
	Ice-melt (+)	0.28	0.28	0.26	0.30	0.27	0.26	0.30	0.29	0.29
Mean volume (μm^3)	Ice-melt (−)	0.03	0.04	0.03	0.04	0.04	0.04	0.03	0.04	0.04
	Ice-melt (+)	0.02	0.02	0.04	0.04	0.02	0.03	0.04	0.05	0.04
CCC (fg C cell^{-1})	Ice-melt (−)	10.7	13.7	10.6	12.1	12.4	13.1	11.1	13.7	14.7
	Ice-melt (+)	7.9	8.9	14.5	13.1	7.5	9.1	14.2	15.3	13.2
Cocci (%)	Ice-melt (−)	71.2	71.2	52.9	56.3	71.7	47.4	66.7	56.4	50.5
	Ice-melt (+)	68.5	68.3	32.1	65.0	68.5	57.1	53.0	39.9	51.2
Rods (%)	Ice-melt (−)	16.9	13.6	25.9	26.4	11.3	27.8	19.4	24.8	25.2
	Ice-melt (+)	9.3	11.7	14.9	9.4	17.4	4.8	28.0	14.0	15.2
Vibrios (%)	Ice-melt (−)	5.1	3.0	4.7	6.9	5.7	12.4	2.2	2.6	6.8
	Ice-melt (+)	3.7	8.3	17.9	6.0	2.2	1.9	6.8	16.9	14.4
Spirillae (%)	Ice-melt (−)	0.0	0.0	0.0	0.0	0.0	0.0	0.0	1.7	1.9
	Ice-melt (+)	0.0	0.0	0.0	0.0	0.0	0.0	0.0	2.8	0.0
Coccobacilli (%)	Ice-melt (−)	3.4	3.0	10.6	8.0	7.5	7.2	6.5	6.8	10.7
	Ice-melt (+)	5.6	0.0	0.0	0.0	4.3	0.0	3.8	4.5	2.4
Curved rods(%)	Ice-melt (−)	3.4	9.1	5.9	2.3	3.8	5.2	5.4	7.7	4.9
	Ice-melt (+)	13.0	11.7	35.1	19.7	7.6	36.2	8.3	21.9	16.8

Cell carbon content (CCC), dependent on cell volume, varied between 2.2 and 37.2 with a mean value of 12.3 ± 9.2 fg C cell^{-1} without any significant difference between the investigated periods. As well as for cell volumes, CCC were higher at the brackish stations than at riverine ones (about 13 fg C cell^{-1}). PB was in a range of 2.3–41 μg C L^{-1} in Ice-melt (−) (St. 9) and Ice-melt (+) (St. 7), respectively. It varied between the two periods and was 2.6 times higher in July (21 μg C L^{-1}) than in May (8.4 μg C L^{-1}). The highest values were found in July, particularly at the brackish stations (Figure 2).
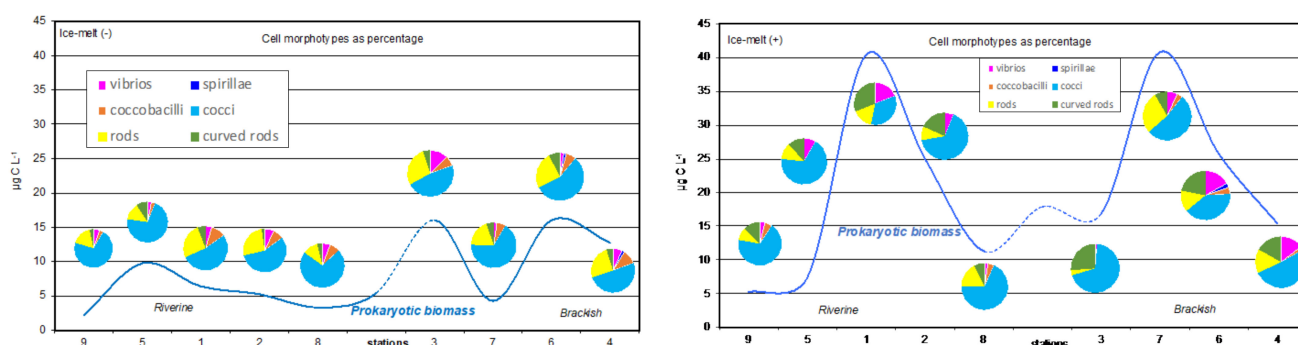

Figure 2. Distribution of prokaryotic biomass (line in blue) and abundance as a percentage of the total morphotypes at the riverine and brackish stations of the Pasvik River during the two seasonal samplings. May, Ice-melt (−); July, Ice-melt (+).

On the whole, remarkable small cocci represented, on average, about 60% (range: 32–71%) of total abundance, thus being the dominant morphotype at all stations and periods (Figure 2). In Ice-melt (−), they were followed by rods (19%), while vibrios, coccobacilli, and curved rods occurred in a small percentage (about 5% of the total cells). Finally, spirillae, observed only at brackish stations, were fairly negligible. Differently, in the Ice-melt (+) period, curved rods represented the second frequent morphotype (on average the 18% of the total) with a higher

percentage at the brackish stations. Rods and vibrios accounted, on average, for 14 and 9%, respectively, and spirillae and coccobacilli were almost lacking.

3.4. Microbial Activity Measurements

3.4.1. Extracellular Enzymatic Activity

Results highlighted different gradients of microbial activities, with different pathways of carbon and phosphorous in the different sampling sites (Figure 3a). Higher values of GLU and AP were generally recorded in Ice-melt (−), whereas LAP activities were higher in Ice-melt (+). In Ice-melt (−), the lowest LAP rates were measured at riverine stations. Conversely, GLU and AP reached their high maximum rates at the riverine St. 5; high values were also found at the brackish St. 7 and St. 4, while the lowest rates were measured at stations St. 1 and St. 3, located in the riverine and brackish area, respectively. In Ice-melt (+), the lowest LAP rates were recorded at riverine St. 8. The maximum value of both GLU and AP was measured at brackish St. 4, and the minimum at St. 2.
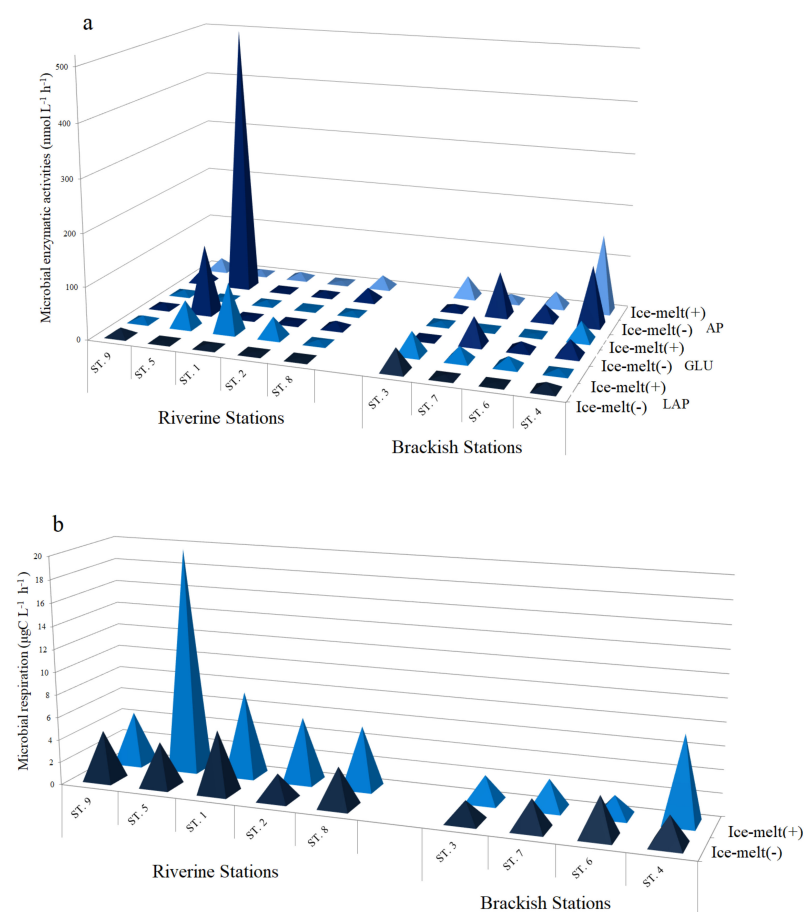

Figure 3. Microbial activities in water samples from the Pasvik River. (**a**) Enzymatic activities; (**b**) respiratory activity.

3.4.2. Respiratory Activity

Microbial respiration in water samples was higher in Ice-melt (+) than in the Ice-melt (−) period. The lowest and highest values were recorded at brackish St. 3 and riverine St. 1 in Ice-melt (−), and at brackish St. 6 and riverine St. 5 during Ice-melt (+), respectively (Figure 3b). Globally, the microbial respiration rate increased in the Ice-melt (+) period at almost all stations, with particular evidence for riverine St. 5 whose values of $\mu gC\ L^{-1}\ h^{-1}$ increased from 3.9 in Ice-melt (−) to 19.8 in the Ice-melt (+) season.

3.5. Phylogenetic Composition of the Bacterial Community

Main data on total sequence reads, quality trimming, OTU information, and diversity indices obtained for water samples are summarized in Supplementary Table S1. The phylogenetic composition of the bacterial community is shown in Supplementary Figure S2. In the Ice-melt (−) season (Figure 4a), Proteobacteria was mainly represented. Among them, Gammaproteobacteria were more abundant at riverine St. 9, St. 1, and St. 8 with a relative abundance of 31.6, 75.4, and 40.8% of the total community, respectively. Differently, Alphaproteobacteria dominated the communities of brackish St. 3, St. 4, and St. 6 with a relative percentage of 63.7, 50.2, and 68.9% of the total community, respectively. Among other well-represented groups, Bacteroidetes were almost equally distributed among stations, with the highest relative abundance at the brackish St. 7 (20.5% of the total community). Cyanobacteria generally ranged between 0.5 (riverine St. 1) and 13.7% (St. 6), with the exception of St. 7 where they accounted for the 40.6% of the total community. Actinobacteria and Firmicutes contributed to the bacterial community to a lesser extent and were best represented at riverine St. 9. The relative abundance of the remaining phyla (i.e., Planctomycetes, Chloroflexi, Deinococcota, Delsufobacterota, Patescibacteria) was generally less than 1% in all samples.
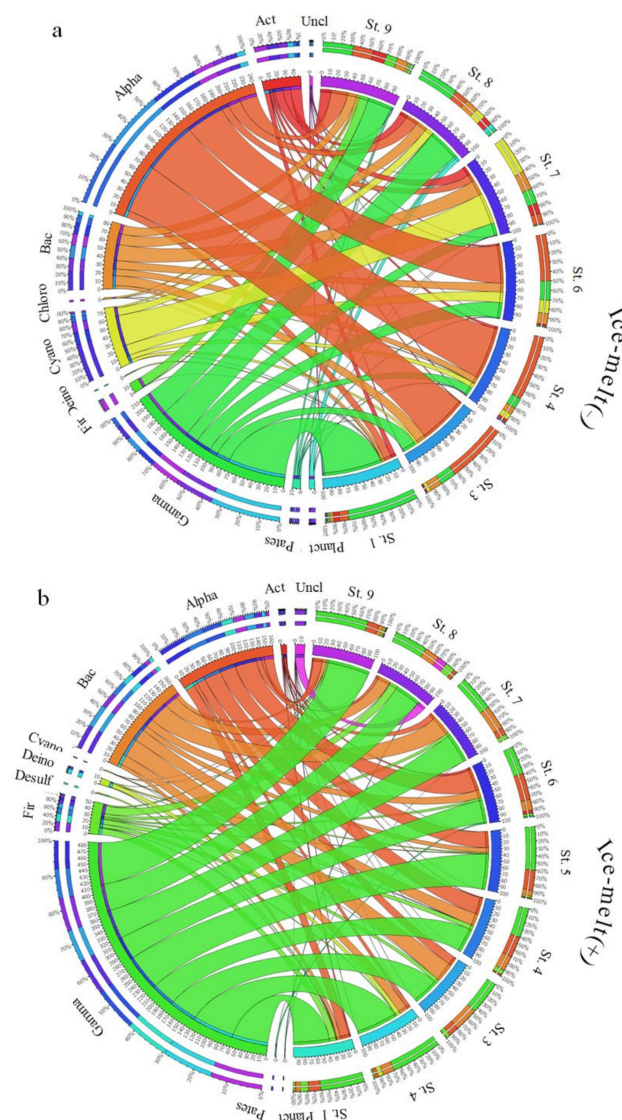

Figure 4. Circle tables evidencing phylogenetic groups detected at each sampling site during Ice-melt (−) (**a**) and Ice-melt (+) (**b**) seasons in the Pasvik River.

In the Ice-melt (+) period (Figure 4b), Gammaproteobacteria dominated the bacterial communities of all water samples, followed by Alphaproteobacteria and Bacteroidetes. The relative abundance of Gammaproteobacteria was slightly lower at brackish stations (39.2% and 41.1% of the total community at St. 6 and St. 4, respectively), while at the riverine stations, it ranged between 45.5 (St. 8) and 71.8% (St. 9). Conversely, Alphaproteobacteria were more abundant at the riverine stations, with relative percentages ranging from 9.6% to 37.3% of the total bacterial community at St. 7 and St. 6, respectively. Bacteroidetes were more abundant at brackish St. 3 and St. 7, with values of 32.9 and 34.2% of the total communities, respectively. Actinobacteria contributed to the bacterial communities to a lesser extent in the Ice-melt (+) period (maximum value of 3.8% at St. 6). Minor groups showed percentages less than 1% at all stations. Exceptions were Deinococcota (7% at riverine St. 2) and Patescibacteria (1.9% at brackish St. 6). No significant differences have been detected by one-way ANOVA between relative abundance values, both within the same season and between the two seasons.

Overall, a total of 63 genera were retrieved at a relative abundance >1%. Among Bacteroidetes, the genus *Flavobacterium* predominated in Ice-melt (−) (May), with abundance ranging between 2.38 and 11.25% (St. 1 and St. 7, respectively). Differently, the same phylum was better represented by the genera *Gillisia* (max value 32.5% at St. 3) and *Hymenobacter* (max value 20.5% at SP2-7) in Ice-melt (+) (July). Within *Firmicutes*, the genus *Geobacillus* was the most represented in Ice-melt (−) at St. 9 (9.0% of the total community), while *Exiguobacterium* dominated the community in Ice-melt (+) at St. 1 and St. 8 (11.1 and 14.2%, respectively). *Paenisporosarcina*, *Psychrobacillus,* and *Staphylococcus* were present at low abundances in Ice-melt (+) at St. 3, St. 4, and St. 6. Among Betaproteobacteria, the genera *Rhodoferax*, *Polaromonas,* and *Massilia* dominated the bacterial community in Ice-melt (−) and were retrieved with the highest abundances at St. 1 (20.7, 13.6, and 12.2% of the total community, respectively).

In particular, members of the genus *Massilia* were detected with an increased relative abundance at brackish St. 1, St. 2, and St. 5 in Ice-melt (+) (45.1, 59.6, and 43%, respectively). In the same period, among Gammaproteobacteria, the genus *Psychrobacter* was particularly abundant at St. 3, St. 4, and St. 7, accounting for 44.9, 35.9, and 49.8% of the total community, respectively. At St. 6, 30.4% of the bacterial community was represented by members of the genera Escherichia-Shigella (Figure 5).

Figure 5. Bubble scatter plot of phylogenetic groups detected at each sampling site during the two sampling campaigns in the Pasvik River.

OTU-sharing between Ice-melt (−) and Ice-melt (+) conditions for riverine and brackish samples is shown in Supplementary Figures S3 and S4. The highest percentage of shared OTUs was retrieved between riverine and brackish sites at the beginning of the ice melting season (20.5%), otherwise the lowest number of shared OTUs was found for brackish sites in the two different ice-melting seasons (11.4%). A very low percentage of shared OTUs was observed among sites, with the highest value retrieved among samples of the riverine area in the Ice-melt (−) season (6.6%) and the lowest in the same area, but during the Ice-melt (+) season (2.9%).

3.6. Statistical Analyses

As a first step, we carried out the statistical analysis separately for the samples from Ice-melt (−) and Ice-melt (+) seasons and by considering the different kind of data: Environmental, biological (microbial counts and activities), and phylogenetic composition. The spatial distribution of stations in the two periods showed a different configuration, in which the strongest contribute to the components was provided by salinity, TSM, POC, and TDS values in the Ice-melt (+) samples. In both cases, the brackish stations did not group together. As it is shown by the PCA in Figure 6a in Ice-melt (−), the two main components explained 78.7% of the total variance, with the first component explaining 47.5% of the total variance, mainly influenced by PIC concentration, and the second component accounting for 31.2% and influenced mainly by TDS (negatively correlated). Two main clusters occurred: A larger one grouping brackish St. 6 and St. 7 (forming a sub-group), and riverine St. 1, St. 5, and St. 9 (forming a subcluster in which St. 1 and St. 5 is grouped together in a subgroup), and a smaller one including brackish St. 3 and St. 4. Riverine St. 2 and St. 8 appeared isolated.

Figure 6b shows the PCA of samples collected in Ice-melt (+) conditions. The two main components explained 81% of the total variance, with the first component explaining 52.3% of the total variance, mainly influenced by salinity, and the second component accounting for 28.7% and influenced mainly by TSM and POC (positively correlated) and TDS (negatively correlated) values. Three different clusters occurred: One grouping riverine St. 1 and St. 5, and a second cluster including brackish St. 4 and riverine St. 2.
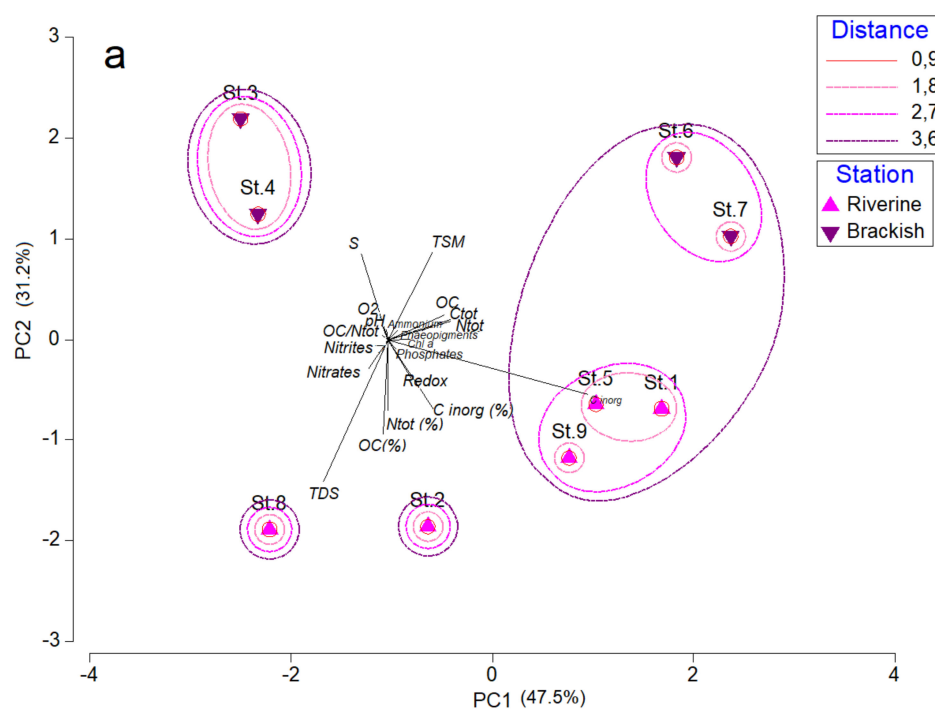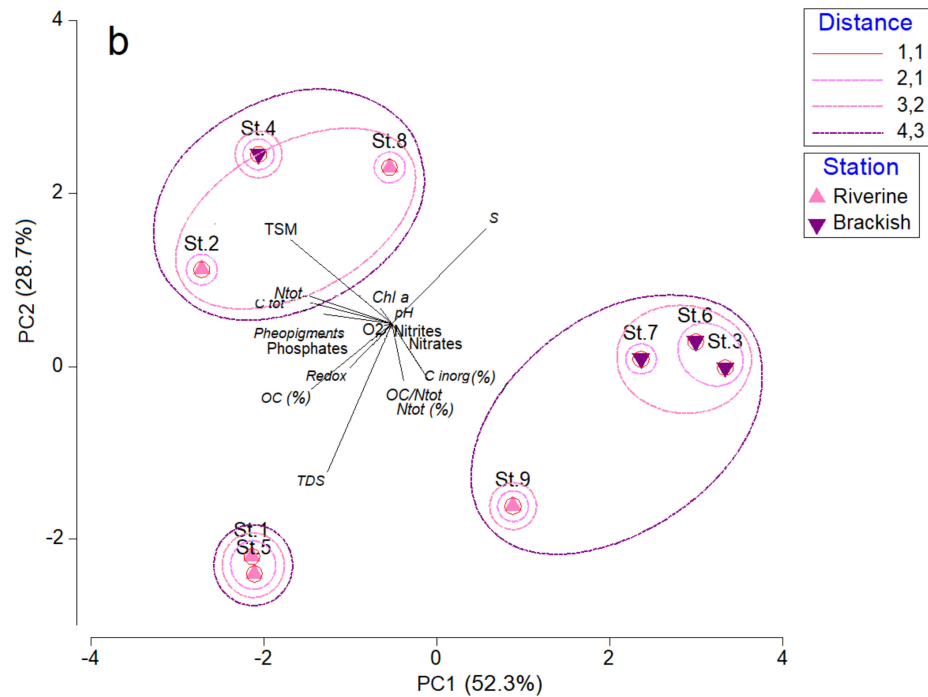

Figure 6. *Cont.*

Figure 6. Principal Component Analysis (PCA) computed on Euclidean distance calculated with environmental parameters data recorded for each sampling point along the Pasvik River in Ice-melt (−) (**a**) and Ice-melt (+) (**b**).

As shown in the nMDS in Figure 7, on which vectors from diversity data were superimposed, in Ice-melt (−),riverine St. 1 fully separated from all the other stations, grouping together in a unique cluster with a similarity of 80% (Figure 7a). The same analysis applied to data from Ice-melt (+) showed a complete separation of St. 5 (Figure 7b).
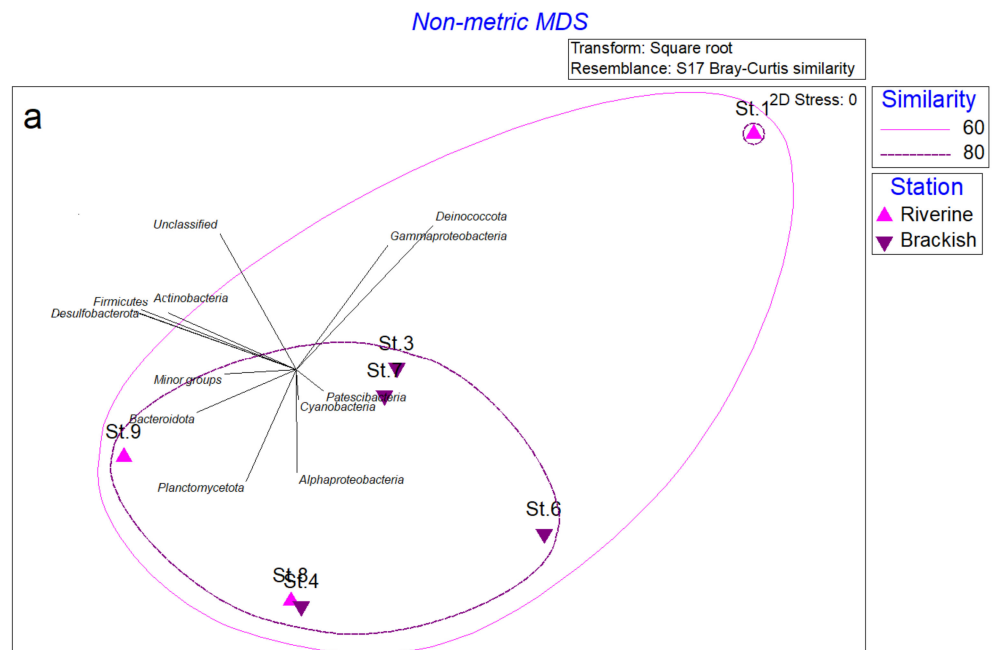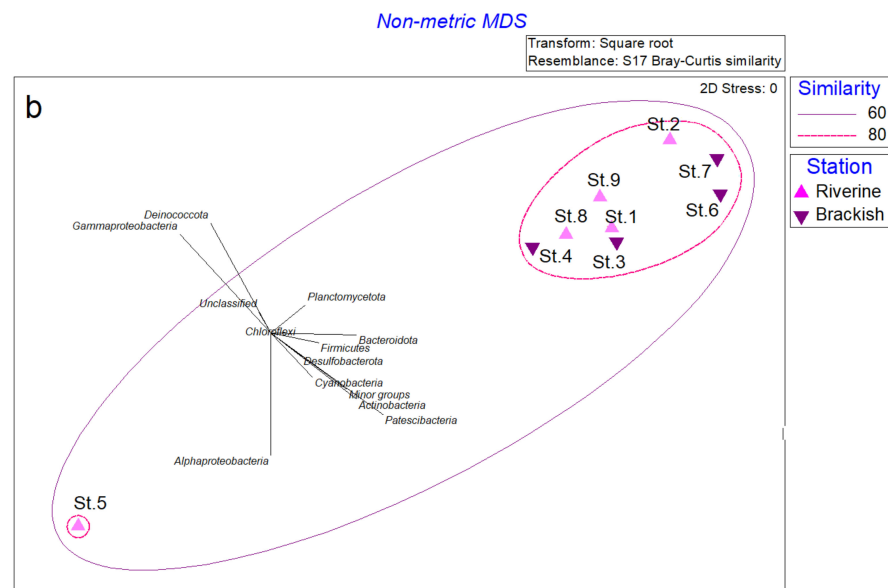

Figure 7. *Cont.*

Figure 7. nMDS analysis computed on biological data obtained for the microbial communities from the Pasvik River water at each sampling point in Ice-melt (−) (**a**) and Ice-melt (+) (**b**) seasons.

Figure 8, referring to abundance data at the phylum level in Ice-melt (−) and Ice-melt (+) conditions, showed a clear spatial separation of the samples taken during the two periods; while samples from the Ice-melt (+) period spread to a shorter distance than each other, samples from Ice-melt (−) appeared more dislocated and formed a single cluster including brackish St. 3, St. 4, and St. 6. Stations from the Ice-melt (+) season formed three small clusters with a similarity of 80%, organized as follows: Riverine St. 1 and St. 9; brackish St. 4 and St. 6; brackish St. 3, St. 7, and riverine St. 8. A significant difference was highlighted in relative abundance by the ANOSIM test computed by imposing "season" (Ice-melt (−) and Ice-melt (+)) as factors (Global R = 0.6; p = 0.001), and the SIMPER analysis attributes this difference mainly to Bacteroidetes and Actinobacteria abundances with cumulative values of 77.6% and 68.7%, respectively.
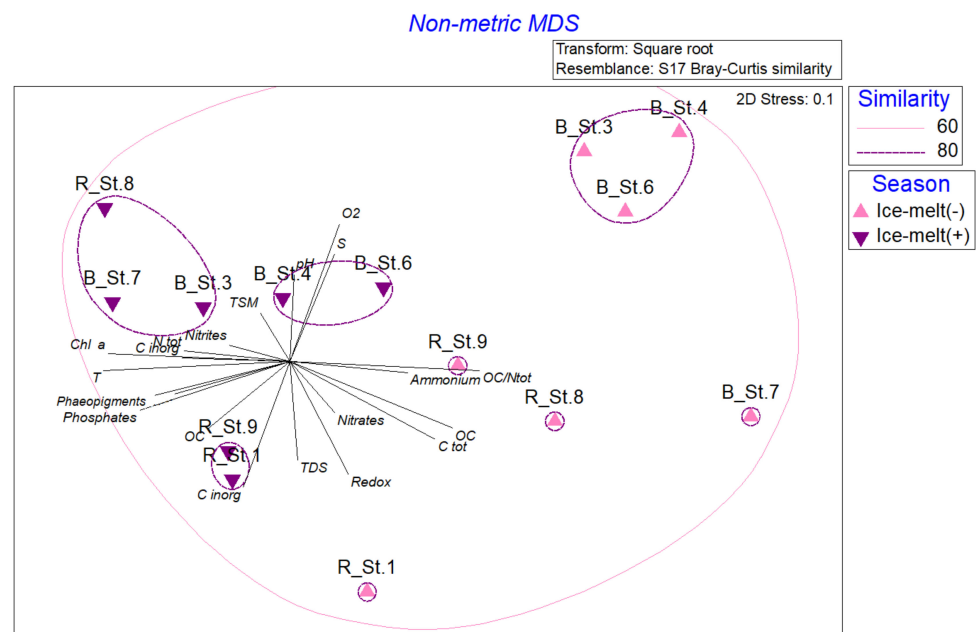

Figure 8. nMDS computed on the relative abundance of phyla detected in both Ice-melt (−) and Ice-melt (+) in the Pasvik River at each sampling point.

4. Discussion

The Arctic plays a key role in the global Earth's climate system. Warming effects deriving from climate change processes are expected to be more and more pronounced at high latitudes, where most of the global carbon pool is stored [31,32] with worrying effects on the entire ecological system, impacting physical, biogeochemical, and ecological levels (e.g., populations dynamics and food web interactions) [4]. The pivotal role that microbial communities exert at biogeochemical cycles and trophic chain levels in aquatic ecosystems is even more noticeable in this sensitive area, in which climate changes could strongly affect microbial activities [33,34]. A deeper understanding of how perturbations related to climate change affect ecological dynamics at the microbial level (e.g., structure and functions) can contribute to prospect on how the ecosystem could react in the coming decades. In this study, a survey on physical-chemical parameters, functional, and diversity traits of Arctic microbial communities is proposed in a perspective of more or less advanced state of ice melting, thus mentioned as Ice-melt (−) and Ice-melt (+) seasons. This study aimed to verify the changes inducted by ice-melting processes, by assuming that a greater similarity between riverine and brackish areas will occur at higher levels of hydrological riverine connectivity.

From a physical-chemical point of view, no statistically significant differences were highlighted between riverine and brackish stations, nor between the Ice-melt (−) and Ice-melt (+) periods. In both cases, salinity and total dissolved solids values were respectively higher and lower in brackish stations than in riverine ones, probably due to a more direct effect of ice melting and terrestrial inputs on them (Tables 1 and 2). The lowest δ^{13} POC values occurring in the samples collected in riverine stations (Table 2) seems to confirm a terrestrial origin of organic matter since, in general, terrestrial organic material is isotopically depleted in δ^{13} POC values compared to marine organic matter [35]. According to the environmental assessment (Figure 6), the separation between brackish and riverine stations appeared more pronounced during the Ice-melt (−) period, while a more dispersed distribution occurred during the Ice-melt (+) period, by indicating a change in the physical-chemical configuration along the sites.

The ratio between chlorophyll-a and phaeopigments, on average around 60–70%, indicates moderate photosynthetic activity at both sampling times. However, if during Ice-melt (−) high values of GLU and AP activities (Figure 3a) suggest a relation to photosynthetic production, during the Ice-melt (+) period, higher LAP activities indicate the occurrence of fresh labile compounds, probably deriving from ice melting related to a summer temperature increase and river inputs. An increase in enzymatic activity rates in relation to the release of organic matter from ice melting was also observed along a transect within Kongsfjorden (Svalbard) in May 2016 [36], confirming that organic carbon sources stimulate the microbial community to produce enzymes to decompose the available organic polymers. Moreover, as observed in coastal to off-shore gradients [37,38], increased runoff not only affects the organic matter pool but also changes the dynamics of coastal bacterial communities with a shift toward a higher influence of riverine bacteria, with implications on the metabolic profiles and organic matter degradation capability of such communities. Similar to enzymatic activities, respiratory activity (Figure 3b), as a biochemical proxy of the potential metabolic activity, was higher at Ice-melt (+) than Ice-melt (−) conditions. Overall, these findings suggest an active biogeochemical cycling along the Pasvik River, especially in the Ice-melt (−) period.

To our knowledge, quantitative data on the prokaryotic cells, in terms of abundance, size, biomass, as well as on their morphology have so far been lacking for the Pasvik River. The microbial abundance and morphometric analysis showed a spatial diversification between the riverine and brackish stations (Table 4 and Figure 2). The number and the biomass of the prokaryotic cells decreased from the riverine towards the outer parts of the river. Moreover, a temporal change was observed with the highest values of prokaryotic abundances and biomass in Ice-melt (+) at the stations adjacent to the Bay in front of Pajusaari islet and Kirkenes Harbour (St. 1 and St. 7). Prokaryotic abundance estimated by

Image analysis (in the range 10^5–10^6 cells mL^{-1}) was lower than that found by Gladyshev et al. [39], in a study carried out in the Siberian Yenisei River, and similar to that observed by Ortega-Retuerta et al. [40], in the Canadian Arctic.

Interestingly, in all samples, the prokaryotic community showed cell sizes smaller than 0.1 μm^3. These cells could be classified as ultramicrobacteria (UMB), i.e., species that maintain their size and volume regardless of their growth condition [41], or ultramicrocells, i.e., cells that reduce their size and volume as a consequence of life cycle changes or of extreme environmental factors [42]. Temporary size reduction of cells has been observed in natural samples and laboratory studies, as strategies to maintain cell integrity and function in response to unfavorable environmental factors [43,44]. Moreover, the high surface-to-volume ratios of small cells could be due to an adaptive strategy to low nutrient concentrations [45]. The morphotypic structure was characterized by very small cocci that overwhelmed any other cell type. A speculative approach would suggest that cocci exhibited an efficient reproductive strategy. Large cells were seldom seen and contributed generally less than 1% of the total cells. Their presence, particularly in the brackish stations, however, could suggest a higher content of organic matter.

During the Ice-melt (+) season, the bacterial communities (riverine vs. brackish stations) were more similar than during the Ice-melt (−) season according to the morphological and functional data retrieved in the Pasvik area, as shown Figure 7. This observation suggests a potential effect of mixing of communities due to the ice-melting processes.

A decrease in microbial diversity from the riverine to the most marine sites was recently reported by Papale et al. [13] during an Ice-melt (+) sampling (June 2013) in the same area. In line with this, here the richness (in terms of OTU number) also showed a decrease from the riverine to the brackish stations in both periods, but a reduction of OTUs was also more evident in the Ice-melt (−) than in the Ice-melt (+) season, probably due to effects of runoff waters from melting.

The correlation between the increasing runoff and the decreasing in taxonomic and functional diversity of microbial communities was also found in freshwater systems. Ruiz-González et al. [8] and Niño-García et al. [9], observed a decrease in microbial diversity along boreal rivers, supporting the hypothesis that variations in runoff volumes may affect local sorting of bacteria with a common origin from a highly diverse terrestrial community. During the Ice-melt (−) period, a different dominance of Gammaproteobacteria and Alphaproteobacteria was observed in riverine and brackish stations, respectively. Conversely, during the Ice-melt (+) period, a more pronounced homogeneity was evidenced, with comparable abundance values in the magnitude order Gammaproteobacteria > Alphaproteobacteria > Bacteroidetes. Although the microbial communities were not completely affected in terms of composition in bacterial phyla, some variations occurred with the increasing melting of the ice, leading to a different structure (Figure 4).

The different structure of the communities at the genus level in the two sampling periods is noteworthy (Figure 5). Indeed, while the genera *Flavobacterium* (Bacteroidetes) and *Geobacillus* (Firmicutes) dominated the Ice-melt (−) community, the same phyla were better represented by *Gillisia*, *Hymenobacter,* and *Exiguobacterium* in the Ice-melt (+) period. In particular, the *Cytophaga-Flavobacterium* is a taxonomic group of Bacteroidetes, which is generally reported as dominant in aquatic systems, including rivers and lakes [46,47], with a pivotal role in the utilization of organic material [48]. *Flavobacterium* members were mostly detected in the riverine and brackish stations during the Ice-melt (−) season, when the organic matter starts to be available with the beginning of melting processes. In line with this, detected flavobacterial phylotypes might be correlated to phytoplankton blooms, with the progressive utilization of fresh phytodetritus [49,50]. As obligate thermophiles, *Geobacillus* species might have been expected to be found only in the warmest sites (e.g., equatorial deserts, geothermal and hydrothermal springs). However, as a paradox, *Geobacillus* has already been isolated in anomalously high numbers even from cold places of the Earth, such as cool soils and permanently cold ocean sediments [51]. Among Firmicutes, *Exiguobacterium* replaced the genus *Geobacillus* in Ice-melt (+) conditions. The

occurrence of such a cosmopolitan genus spans from marine environments and freshwaters to permafrost and hot springs, being able to grow in a wide range of temperature, pH, salinity, and heavy-metal concentrations. Comprehensive capacity of diverse polysaccharides utilization and environmental stress resistance are at the basis of its survival and extensive distribution. *Exiguobacterium* was proposed as a valuable model for studying the adaptive strategy of bacteria in a changing environment [52].

The microbial community composition at the genus level also reflected the occurrence of taxonomic groups widely distributed in Arctic aquatic systems, e.g., the case of *Polynucleobacter* and *Limnohabitans*, but also the presence of taxonomic groups of more pronounced terrigenous origin, which suggest the influence of ice-melting processes. *Polynucleobacter* and *Limnohabitans* are two typically freshwater genera [53,54], also recently retrieved in the Pasvik river water and sediments, with higher abundances in water samples [13]. In support of this assumption, bacterial members of the genera *Massilia*, previously found in Arctic sediments and glacier permafrost [55,56], were detected at a higher percentage just at the riverine stations in the period of Ice-melt (+), which realistically had a more direct influence from the fluvial inputs. The genus *Hymenobacter,* detected here only in riverine and brackish stations during the Ice-melt (+) season, was recently isolated from soil of the Arctic station Spitsbergen (Svalbard, Norway) [57], but it was also obtained from glacier ice environments [58] and permafrost [59]. Finally, *Acinetobacter* members, here retrieved in the riverine stations during the Ice-melt (+) season, are typically associated with Arctic fjords [60] and were found also in glacial snow and ice in mountainous locations outside the Arctic [61].

The strong difference at the phylogenetic level between communities occurring during the two seasons is more remarkable in Figure 8, where the stations from Ice-melt (+) appeared closer to each other than the stations of the Ice-melt (−) period. Globally, all the observations obtained at different scales analyzed here (namely physical-chemical, biological, and taxonomical ones) suggested a different arrangement of riverine and brackish stations during the two periods, evidencing a clear influence of the melting process.

5. Conclusions

The attention that in recent years has been focused on issues related to climate change at a global level requires transversal efforts in research to adopt remedial solutions. Here, we report a wide-embracing survey of hydrology, biochemistry, and microbiology of the Pasvik River, with a double check of spatial and temporal variations in the attempt to verify the starting assumption, namely that a higher hydrological connectivity due to ice melting would have generated a major homogeneity within upland and lowland microbial communities. Data confirmed our hypothesis while additionally providing other novel insights that could be used in the future for long-term investigations of the Arctic area.

Supplementary Materials: The following are available online at https://www.mdpi.com/article/10.3390/w13162297/s1, Figure S1: Distribution of chlorophyll-a (chla; line in green) and phaeopigments (phaeo; line in red) concentrations, and percentage of size-fractions (micro-, nano- and pico-phytoplankton) at the riverine and brackish stations of the Pasvik River during the two seasonal sampling. May, Ice-melt (−); July, Ice-melt (+); Figure S2: Phylogenetic groups retrieved in May (Ice-melt (−)) and July (Ice-melt (+)), at each sampling site along the Pasvik River; Figure S3: Venn diagrams showing the OTU-sharing between Ice-melt (−) and July (Ice-melt (+) conditions and areas (riverine and brackish): (a) Riverine and brackish stations in Ice-melt (−); (b) riverine and brackish stations in Ice-melt (+); (c) riverine stations; (d) brackish stations; (e) all season/site groups; Figure S4: Venn diagrams representing OTU-sharing between samples: (a) Riverine stations in May; (b) riverine stations in July; (c) brackish stations in May; (d) brackish stations in July. Table S1: Total number of sequence reads, good-quality reads, observed numbers of OTUs, Shannon diversity, Evenness and Chao 1 indices per sample of the bacterial 16S rRNA gene data sets.

References

1. Bring, A.; Fedorova, I.; Dibike, Y.; Hinzman, L.; Mård, J.; Mernild, S.H.; Prowse, T.; Semenova, O.; Stuefer, S.L.; Wooet, M.-K. Arctic terrestrial hydrology: A synthesis of processes, regional effects and research challenges. *J. Geophys. Res. Biogeosci.* **2016**, *121*, 621–649. [CrossRef]
2. Hauptmann, A.L.; Markussen, T.N.; Stibal, M.; Olsen, N.S.; Elberling, B.; Baelum, J.; Sicheritz-Pontén, T.; Jacobsen, C.S. Upstream freshwater and terrestrial sources are differentially reflected in the bacterial community structure along a small Arctic river and its estuary. *Front. Microbiol.* **2016**, *7*, 1474. [CrossRef] [PubMed]
3. Williamson, C.E.; Saros, J.E.; Vincent, W.F.; Smol, J.P. Lakes and reservoirs as sentinels, integrators, and regulators of climate change. *Limnol. Oceanogr.* **2009**, *54*, 2273–2282. [CrossRef]
4. Colby, G.A.; Ruuskanen, M.O.; St. Pierre, K.A.; St. Louis, V.L.; Poulain, A.J.; Aris-Brosou, S. Climate change lowers diversity and functional potential of microbes in Canada's high Arctic. *bioRxiv* **2019**, 705178. [CrossRef]
5. Dinasquet, J.; Ortega-Retuerta, E.; Lovejoy, C.; Obernosterer, I. Editorial: Microbiology of the Rapidly Changing Polar Environments. *Front. Mar. Sci.* **2018**, *5*, 154. [CrossRef]
6. Sipler, R.E.; Kellogg, C.T.E.; Connelly, T.L.; Roberts, Q.N.; Yager, P.L.; Bronk, D.A. Microbial community response to terrestrially derived dissolved organic matter in the coastal Arctic. *Front. Microbiol.* **2017**, *8*, 1018. [CrossRef]
7. Paulsen, M.L.; Nielsen, S.E.B.; Müller, O.; Møller, E.F.; Stedmon, C.A.; Juul-Pedersen, T.; Markager, S.; Sejr, M.K.; Delgado Huertas, A.; Larsen, A.; et al. Carbon bioavailability in a high Arctic fjord influenced by glacial meltwater, NE Greenland. *Front. Mar. Sci.* **2017**, *4*, 176. [CrossRef]
8. Ruiz-González, C.; Niño-García, J.P.; Del Giorgio, P.A. Terrestrial origin of bacterial communities in complex boreal freshwater networks. *Ecol. Lett.* **2015**, *18*, 1198–1206. [CrossRef] [PubMed]
9. Niño-García, J.P.; Ruiz-González, C.; del Giorgio, P.A. Interactions between hydrology and water chemistry shape bacterioplankton biogeography across boreal freshwater networks. *ISME J.* **2016**, *10*, 1755–1766. [CrossRef]
10. Caputo, S.; Papale, M.; Rizzo, C.; Giannarelli, S.; Conte, A.; Moscheo, F.; Graziano, M.; Aspholm, P.E.; Onor, M.; De Domenico, E.; et al. Heavy metal resistance in bacteria from contaminated Arctic sediment is driven by heavy metal local inputs. *Arch. Environ. Contam. Toxicol.* **2019**, *77*, 291–307. [CrossRef] [PubMed]
11. Cavaco, M.A.; St. Louis, V.L.; Engel, K.; St. Pierre, K.A.; Schiff, S.L.; Stibal, M.; Neufeld, J.D. Freshwater microbial community diversity in a rapidly changing High Arctic watershed. *FEMS Microbiol. Ecol.* **2019**, *95*, fiz161. [CrossRef]
12. Rappazzo, A.C.; Papale, M.; Rizzo, C.; Conte, A.; Giannarelli, S.; Onor, M.; Abete, C.; Cefali, P.; De Domenico, E.; Michaud, L.; et al. Heavy metal tolerance and polychlorinated biphenyl oxidation in bacterial communities inhabiting the Pasvik River and the Varanger Fjord area (Arctic Norway). *Mar. Pollut. Bull.* **2019**, *141*, 535–549. [CrossRef]
13. Papale, M.; Rappazzo, A.C.; Mikkonen, A.; Rizzo, C.; Moscheo, F.; Conte, A.; Michaud, L.; Lo Giudice, A. Bacterial diversity in a dynamic and extreme sub-Arctic watercourse (Pasvik River, Norwegian Arctic). *Water* **2020**, *12*, 3098. [CrossRef]
14. Laganà, P.; Votano, L.; Caruso, G.; Azzaro, M.; Lo Giudice, A.; Delia, S. Bacterial isolates from the Arctic region (Pasvik River, Norway): Assessment of biofilm production and antibiotic susceptibility profiles. *Environ. Sci. Pollut. Res.* **2018**, *25*, 1089–1102. [CrossRef] [PubMed]
15. Tesi, T.; Miserocchi, S.; Acri, F.; Langone, L.; Boldrin, A.; Hatten, J.A.; Albertazzi, S. Flood-driven transport of sediment, particulate organic matter, and nutrients from the Po River watershed to the Mediterranean Sea. *J. Hydrol.* **2013**, *498*, 144–152. [CrossRef]

16. Tesi, T.; Miserocchi, S.; Goñi, M.; Langone, L.; Boldrin, A.; Turchetto, M. Organic matter origin and distribution in suspended particulate materials and superficial sediments from the western Adriatic Sea (Italy). *Estuar. Coast. Shelf Sci.* **2007**, *73*, 431–446. [CrossRef]

17. Strickland, J.D.H.; Parsons, T.R. A practical hand book of seawater analysis. *Fish. Res. Board Can. Bull.* **1972**, *157*, 310.

18. Aminot, A.; Chaussepied, M. Manuel des analyses chimiques en milieu marin. *CNEXO Ed. Jouvre Paris* **1983**, 395.

19. Yentsch, C.S.; Menzel, D.W. A method for the determination of phytoplankton chlorophyll and phaeophytin by fluorescence. *Deep Sea Res.* **1963**, *7*, 221–231. [CrossRef]

20. Lorenzen, C.I. Determination of chlorophyll and phaeopigments spectro-photometric equations. *Limnol. Oceanogr.* **1967**, *12*, 343–346. [CrossRef]

21. Zoppini, A.; Ademollo, N.; Bensi, M.; Berto, D.; Bongiorni, L.; Campanelli, A.; Casentini, B.; Patrolecco, L.; Amalfitano, S. Impact of a river flood on marine water quality and planktonic microbial communities. *Estuar. Coast. Shelf Sci.* **2019**, *224*, 62–72. [CrossRef]

22. Porter, K.G.; Feig, Y.S. The use of DAPI for identifying and counting aquatic microflora. *Limnol. Oceanogr.* **1980**, *25*, 943–948. [CrossRef]

23. La Ferla, R.; Maimone, G.; Azzaro, M.; Conversano, F.; Brunet, C.; Cabral, A.S.; Paranhos, R. Vertical distribution of the prokaryotic cell size in the Mediterranean Sea. *Helgol. Mar. Res.* **2012**, *66*, 635–650. [CrossRef]

24. Hoppe, H.G. Use of fluorogenic model substrates for extracellular enzyme activity (eea) measurement of bacteria. In *Handbook of Methods in Aquatic Microbial Ecology*; Kemp, P.F., Sherr, B.F., Sherr, E.B., Cole, J.J., Eds.; Lewis Publisher: Boca Raton, FL, USA, 1993; pp. 423–432.

25. La Ferla, R.; Azzaro, M.; Maimone, G. Microbial respiration and trophic regimes in the Northern Adriatic Sea (Mediterranean Sea). *Estuar. Coast. Shelf Sci.* **2006**, *69*, 196–204. [CrossRef]

26. La Ferla, R.; Azzaro, M. Microbial respiration in the Levantine Sea: Evolution of the oxidative processes in relation to the main Mediterranean water masses. *Deep Sea Res. Part I* **2001**, *48*, 2147–2159. [CrossRef]

27. La Ferla, R.; Azzaro, M.; Chiodo, G. Microplankton respiratory activity and CO2 production rates in the Otranto Strait (Mediterranean Sea). *Aquat. Ecol.* **1999**, *33*, 157–165. [CrossRef]

28. Bolger, A.M.; Lohse, M.; Usadel, B. Trimmomatic: A flexible trimmer for Illumina sequence data. *Bioinformatics* **2014**, *30*, 2114–2120. [CrossRef]

29. Bolyen, E.; Rideout, J.R.; Dillon, M.R.; Bokulich, N.A.; Abnet, C.C.; Al-Ghalith, G.A.; Alexander, H.; Alm, E.J.; Arumugam, M.; Asnicar, F.; et al. Reproducible, interactive, scalable and extensible microbiome data science using QIIME 2. *Nat. Biotechnol.* **2019**, *37*, 852–857. [CrossRef]

30. Heberle, H.; Meirelles, G.V.; da Silva, F.R.; Telles, G.P.; Minghim, R. InteractiVenn: A web-based tool for the analysis of sets through Venn diagrams. *BMC Bioinform.* **2015**, *16*, 169. [CrossRef] [PubMed]

31. Wagner, D. Microbial communities and processes in Arctic permafrost environments. In *Microbiology of Extreme Soils. Soil Biology*; Dion, P., Nautiyal, C.S., Eds.; Springer: Berlin, Heidelberg, 2008; Volume 13, pp. 133–154.

32. IPCC. *Summary for Policymakers, book section SPM, 1–30*; Cambridge University Press: Cambridge, UK; New York, NY, USA, 2013; Available online: http://www.climatechange2013.org (accessed on 19 August 2021).

33. Melillo, J.M.; Steudler, P.A.; Aber, J.D.; Newkirk, K.; Lux, H.; Bowles, F.P.; Catricala, C.; Magill, A.; Ahrens, T.; Morrisseau, S. Soil warming and carbon-cycle feedbacks to the climate system. *Science* **2002**, *298*, 2173–2176. [CrossRef]

34. Zimov, S.A.; Schuur, E.A.G.; Chapin III, F.S. Permafrost and the global carbon budget. *Science* **2006**, *312*, 1612–1613. [CrossRef]

35. Still, C.J.; Berry, J.A.; Collatz, G.J.; DeFries, R.S. Global distribution of C3 and C4 vegetation: Carbon cycle implications. *Glob. Biogeochem. Cycles* **2003**, *17*, 1006. [CrossRef]

36. Caruso, G.; Madonia, A.; Bonamano, S.; Miserocchi, S.; Giglio, F.; Maimone, G.; Azzaro, F.; Decembrini, F.; La Ferla, R.; Piermattei, V.; et al. Microbial abundance and enzyme activity patterns: Response to changing environmental characteristics along a transect in Kongsfjorden (Svalbard Islands). *J. Mar. Sci. Eng.* **2020**, *8*, 824. [CrossRef]

37. Fortunato, C.S.; Crump, B.C. Bacterioplankton community variation across river to ocean environmental gradients. *Microb. Ecol.* **2011**, *62*, 374–382. [CrossRef]

38. Fortunato, C.S.; Herfort, L.; Zuber, P.; Baptista, A.M.; Crump, B.C. Spatial variability overwhelms seasonal patterns in bacterioplankton communities across a river to ocean gradient. *ISME J.* **2012**, *6*, 554–563. [CrossRef]

39. Gladyshev, M.I.; Kolmakova, O.V.; Tolomeev, A.P.; Anishchenko, O.V.; Makhutova, O.N.; Kolmakova, A.A.; Kravchuk, E.S.; Glushchenko, L.A.; Kolmakov, V.I.; Sushchik, N.N. Differences in organic matter and bacterioplankton between sections of the largest Arctic river: Mosaic or continuum? *Limnol. Oceanogr.* **2015**, *60*, 1314–1331. [CrossRef]

40. Ortega-Retuerta, E.; Jeffrey, W.H.; Babin, M.; Belanger, S.; Benner, R.; Marie, D.; Matsuoka, A.; Raimbault, P.; Joux, F. Carbon fluxes in the Canadian Arctic: Patterns and drivers of bacterial abundance, production and respiration on the Beaufort Sea margin. *Biogeosciences* **2012**, *9*, 3679–3692. [CrossRef]

41. Duda, V.I.; Suzina, N.E.; Polivtseva, V.N.; Boronin, A.M. Ultramicrobacteria: Formation of the concept and contribution of ultramicrobacteria to biology. *Microbiology* **2012**, *81*, 379–390. [CrossRef]

42. Kuhn, E.; Ichimura, A.S.; Peng, V.; Fritsen, C.H.; Trubl, G.; Doran, P.T.; Murray, A.E. Brine assemblages of ultrasmall microbial cells within the ice cover of Lake Vida, Antarctica. *Appl. Environ. Microbiol.* **2014**, *80*, 3687–3698. [CrossRef] [PubMed]

43. Gentile, G.; Maimone, G.; La Ferla, R.; Azzaro, M.; Catalfamo, M.; Genovese, M.; Santisi, S.; Maldani, M.; Macrì, A.; Cappello, S. Phenotypic variations of *Oleispira antarctica* RB8T in different growth conditions. *Curr. Microbiol.* **2020**, *77*, 3414–3421. [CrossRef]

44. La Ferla, R.; Azzaro, M.; Michaud, L.; Caruso, G.; Lo Giudice, A.; Paranhos, R.; Cabral, A.S.; Conte, A.; Cosenza, A.; Maimone, G.; et al. Prokaryotic abundance and activity in permafrost of the Northern Victoria Land and Upper Victoria Valley (Antarctica). *Microb. Ecol.* **2017**, *74*, 402–415. [CrossRef] [PubMed]

45. Young, K.D. The selective value of bacterial shape. *Microbiol. Mol. Biol. Rev.* **2006**, *70*, 660–703. [CrossRef] [PubMed]

46. Giovannoni, S.J.; Rappé, M.S. Evolution, diversity and molecular ecology of marine prokaryotes. In *Microbial Ecology of the Ocean*; Kirchman, D.L., Ed.; Wiley Interscience: New York, NY, USA, 2000; pp. 47–84.

47. Glöckner, F.O.; Fuchs, B.M.; Amann, R. Bacterioplankton compositions of lakes and oceans: A first comparison based on fluorescence in situ hybridization. *Appl. Environ. Microbiol.* **1999**, *65*, 3721–3726. [CrossRef] [PubMed]

48. Kirchman, D.L.; Yu, L.; Cottrell, M.T. Diversity and abundance of uncultured cytophaga-like bacteria in the Delaware estuary. *Appl. Environ. Microbiol.* **2003**, *69*, 6587–6596. [CrossRef]

49. Ngugi, D.K.; Stingl, U. High-quality draft single-cell genome sequence of the NS5 Marine Group from the coastal Red Sea. *Genome Announc.* **2018**, *6*, e00565-18. [CrossRef]

50. Díez-Vives, C.; Nielsen, S.; Sánchez, P.; Palenzuela, O.; Ferrera, I.; Sebastián, M.; Pedrós-Alió, C.; Gasol, J.M.; Acinas, S.G. Delineation of ecologically distinct units of marine Bacteroidetes in the Northwestern Mediterranean Sea. *Mol. Ecol.* **2019**, *28*, 2846–2859. [CrossRef]

51. Zeigler, D.R. The *Geobacillus* paradox: Why is a thermophilic bacterial genus so prevalent on a mesophilic planet? *Microbiology* **2014**, *160*, 1–11. [CrossRef]

52. Zhang, D.-C.; Zhu, Z.; Li, X.; Guan, Z.; Zheng, J. Comparative genomics of *Exiguobacterium* reveals what makes a cosmopolitan bacterium. *bioRxiv* **2020**. [CrossRef]

53. Hahn, M.W.; Kasalicky, V.; Jezbera, J.; Brandt, U.; Jezberova, J.; Simek, K. *Limnohabitans curvus* gen. nov., sp nov., a planktonic bacterium isolated from a freshwater lake. *Int. J. Syst. Evol. Microbiol.* **2010**, *60*, 1358–1365. [CrossRef]

54. Jezberová, J.; Jezbera, J.; Brandt, U.; Lindström, E.S.; Langenheder, S.; Hahn, M.W. Ubiquity of *Polynucleobacter necessarius* ssp. asymbioticus in lentic freshwater habitats of a heterogenous 2000 km^2 area. *Environ. Microbiol.* **2010**, *12*, 658–669. [CrossRef] [PubMed]

55. Son, J.; Lee, H.; Kim, M.; Kim, D.-U.; Ka, J.-O. *Massilia aromaticivorans* sp. nov., a BTEX degrading bacterium isolated from Arctic soil. *Curr. Microbiol.* **2021**, *78*, 2143–2150. [CrossRef] [PubMed]

56. Wang, H.; Zhang, X.; Wang, S.; Zhao, B.; Lou, K.; Xing, X.-H. *Massilia violaceinigra* sp. nov., a novel purple-pigmented bacterium isolated from glacier permafrost. *Int. J. Syst. Evol. Microbiol.* **2018**, *68*, 2271–2278. [CrossRef] [PubMed]

57. Dahal, R.H.; Chaudhary, D.K.; Kim, D.-U.; Kim, J. *Hymenobacter polaris* sp. nov., a psychrotolerant bacterium isolated from an Arctic station. *Int. J. Syst. Evol. Microbiol.* **2020**, *70*, 4890–4896. [CrossRef]

58. Liu, K.; Liu, Y.; Wang, N.; Gu, Z.; Shen, L.; Xu, B.; Zhou, Y.; Liu, H.; Jiao, N. *Hymenobacter glacieicola* sp. nov., isolated from glacier ice. *Int. J. Syst. Evol. Microbiol.* **2016**, *66*, 3793–3798. [CrossRef] [PubMed]

59. Zhang, G.; Niu, F.; Busse, H.-J.; Ma, X.; Liu, W.; Dong, M.; Feng, H.; An, L.; Cheng, G. *Hymenobacter psychrotolerans* sp. nov., isolated from the Qinghai–Tibet Plateau permafrost region. *Int. J. Syst. Evol. Microbiol.* **2008**, *58*, 1215–1220. [CrossRef]

60. Choidash, B.; Begum, Z.; Shivaji, S. Bacterial diversity of Ny-Ålesund, Arctic Archipelago Svalbard. *Mong. J. Biol. Sci.* **2012**, *10*, 67–72.

61. Yang, G.L.; Hou, S.G.; Le Baoge, R.; Li, Z.G.; Xu, H.; Liu, Y.P.; Du, W.T.; Liu, Y.Q. Differences in bacterial diversity and communities between glacial snow and glacial soil on the Chongce ice cap, West Kunlun Mountains. *Sci. Rep.* **2016**, *6*, 36548. [CrossRef]